

FAMILIES OF PERIODIC SINKS: THE QUASI-CONSERVATIVE CASE

FALCOLINI CORRADO, TEDESCHINI-LALLI LAURA

*Dipartimento di Architettura, Università Roma Tre, Via della Madonna dei Monti 40,
I-00184 Rome Italy*

ABSTRACT. We will discuss, as a classical example of dissipative map, the Hénon map when the dissipation vanishes. Using a numerical continuation that we devised, and called “dribbling method” [Falcolini & Tedeschi-Lalli (2013)], one can follow bifurcation paths from the highly degenerate area-preserving case into the dissipative one, organizing families of coexisting attractive periodic orbits with diverging period. The coexistence of sinks is greater and greater approaching the conservative case. When the dissipation parameter goes to zero, we will give numerical evidence of the coexistence of such periodic orbits, in the coordinate and parameter space values. We discuss the dependence of the stability range of periodic orbits with respect to the period. As the period p diverges, we describe here the renormalization scheme we set up to study the families. The families we study all appear as homoclinic bifurcation, and the fixed point causing the homoclinic onset also structures the renormalization scheme. Using the same dribbling method, as further promising application, we also deal with the dissipative Standard map.

1. INTRODUCTION

We will deal with the Hénon system of maps of the plane (x, y) , depending on two parameters a and b :

$$(1) \quad T_{(a,b)}(x, y) := (a - x^2 - b y, x)$$

for values of the constant Jacobian b in the quasi-conservative cases: orientation-preserving $b = 1 - \varepsilon$, and orientation-reversing $b = -1 + \varepsilon$ for very small values of ε . The “historical” Hénon model is orientation reversing, but physicists have found it important to deal with orientation preserving. The two cases differ in various aspects regarding possible bifurcations and their continuation [Hénon(1976)], [Holmes & Whitley, 1984].

A periodic orbit of period p solves $T_{(a,b)}^p(x, y) := (x_p, y_p) = (x, y)$, where $T_{(a,b)}^p(x, y) := T_{(a,b)}(T_{(a,b)}^{p-1}(x, y))$ is the p -th iteration of T . The periodic orbit is therefore linearly attracting if the eigenvalues of its final Jacobian matrix lie inside the unit circle. The Jacobian matrix \mathbf{J} is product of the Jacobian matrix along the orbit $(x_i, y_i), i = 0, \dots, p - 1$:

E-mail address: falco@mat.uniroma3.it, tedeschi@mat.uniroma3.it.

Key words and phrases. Bifurcation curves, Hénon map, Standard Map, renormalization schemes .

$$\mathbf{J} = \prod_{i=0}^{p-1} \begin{pmatrix} -2x_i & -b \\ 1 & 0 \end{pmatrix},$$

At a saddle-node node bifurcation an eigenvalue of \mathbf{J} is exactly 1 whereas it is -1 for a period-doubling bifurcation.

In our paper [Falcolini & Tedeschini-Lalli (2013)] we discuss the orientation reversing case, the coexistence of an increasing number of periodic attractors moving closely towards the singular case $b = -1$; the starting point was a method to “dribble” around the singularities of the bifurcation curves at $b = -1$.

In [Falcolini & Tedeschini-Lalli (2016)] we presented results for the orientation-preserving case $b = 1$ and discussed some global unexpected features of bifurcation curves in the $[b, a]$ parameter plane.

Our “dribbling method” in that cases allowed the study of bifurcation curves, and of their singularity in the limit $|b| \rightarrow 1$ (i.e. $\varepsilon \rightarrow 0$). We detected entire families of periodic orbits sharing a homoclinic geometry.

In this paper we describe the two quasi-conservative cases with further detailed data, in order to discuss our renormalization algorithm with diverging period. As new results we present in both cases ($b = 1$ and $b = -1$) orbits of much larger periods and show that, in the orientation reversing case, the boundaries of their stability range accumulate in an oscillatory fashion as p diverges.

2. THE METHOD FOR STUDYING BIFURCATION CURVES FROM AND INTO THE CONSERVATIVE CASE

Given an initial saddle periodic orbit of period p in the conservative cases, we know that the saddle-node bifurcation curve is singular at $|b| = 1$ so we devised a method to “dribble” this singularity. The crucial observation is that saddles are robust, so can always be continued into the dissipative regime. Once in the dissipative regime, one can look for the companion node, that necessarily exists (see [Falcolini & Tedeschini-Lalli (2013)] for details and arguments).

At each \bar{b} where the p -orbit still exists, we detect the value of $a_{sn}(\bar{b})$ at which the saddle-node appears and the value of $a_{pd}(\bar{b})$ for which the periodic orbit first double its period (see Fig.1).

Such values lie on curves in space (b, a) , which can then be evaluated with a continuation method in the four variables (x, y, a, b) see for instance, [Kuznetsov, 1999].

Now all is set, to study the singularity of the curves $a_{sn}(b)$, $a_{pd}(b)$ as $|b| \rightarrow 1$, which we did in the previously cited papers.

We want to study families of orbits sharing a common geometry. So we initialize the search of a family of periodic orbits with increasing period. We start with a saddle orbit of short period p at one of the area preserving cases, $|b| = 1$. The advantage of starting with a low period is that orbits and their spatial patterns are usually easier to detect (see Fig.2).

$$b \in (-1, -0.95], \quad p = 14$$

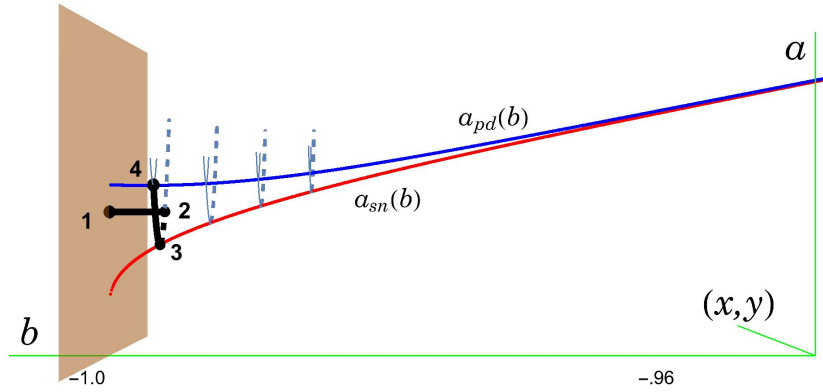


FIGURE 1. Dribbling a singularity and then approaching it. (1) Start from $b = -1$ at a chosen value of \bar{a} with a period- p saddle point. Follow the orbit in $|b| < 1$ up to an arbitrary \bar{b} using a continuation method for (x, y, b, \bar{a}) . (2) Follow the saddle branch, moving downward in a , for (x, y, \bar{b}, a) up to the value $a_{sn}(\bar{b})$ marked with (3). Follow the node branch, moving upward in a , for (x, y, \bar{b}, a) up to the first period-doubling value $a_{pd}(\bar{b})$ marked with (4)

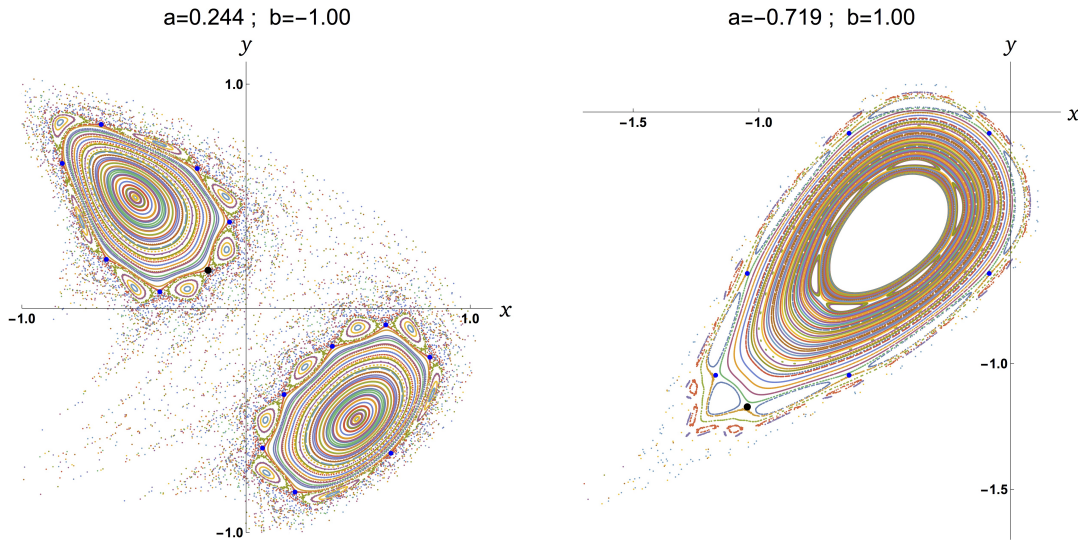


FIGURE 2. The conservative cases: example of an initial saddle periodic orbit for $b = \pm 1$. Left: for $b = -1$ and $a = 0.244$ the big dots represent a period 14 orbit. Right: for $b = 1$ and $a = -0.719$ the big dots represent a period 7 orbit

We then follow the method described above, to detect bifurcation curves depending on p . We follow the periodic orbit into $|b| < 1$ till a value of $b = \bar{b}$ for which the orbit still exists. We then find the precise a values, depending on \bar{b} and p , at which the orbit appears ($a_{sn}(\bar{b})$) and at which it first double its period ($a_{pd}(\bar{b})$) (these values exist in this case, as for [Yorke & Alligood, 1985]). We finally use a continuation method to follow the stability range of the periodic orbit for $|b| \rightarrow 1$. Each curve in fact also depends on period p . Overlapping of stability ranges for different period p in $[b, a]$ plane, signal areas of parameters that allow coexistence of sinks.

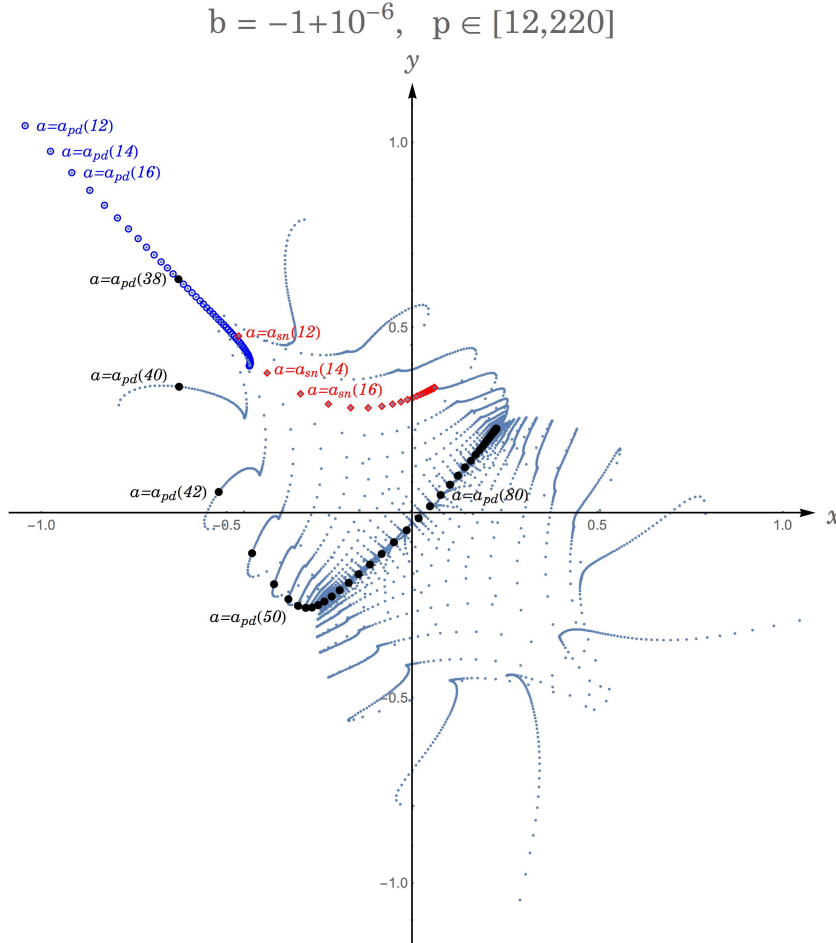


FIGURE 3. Space displacements of the orbits for the case $b = -1 + 10^{-6}$ for $a_{sn}(p)$ and $a_{pd}(p)$ with p in the range $[12, 220]$. The diamonds contain initial points of saddle-node periodic orbits at their formation for $a = a_{sn}(p)$ whereas the circles contain initial points at their first doubling for $a = a_{pd}(p)$. For period doubling initial points at increasing values of p , the algorithm follows the blue circled branch for low periods and the black large dots for larger periods.

3. LARGE PERIODS: A RENORMALIZATION SCHEME IN p .

The families of curves we study, regard sinks that arise via homoclinic bifurcations; all sinks are therefore geometrically organized in families according to the homoclinic connection.

In Fig.3 we report the spatial configuration of a family of saddle–nodes. Note the space displacement of the orbit for different values of $a_{sn}(p)$ and $a_{pd}(p)$ as a function of p .

We would like to follow such study in two different variables: both increasing the period p , keeping b fixed, and also varying b keeping the period p fixed. At varying $|b| \rightarrow 1$, one can study the actual nature of the singularity of the bifurcation curves, attained at the conservative case, as we did in [Falcolini & Tedeschini-Lalli (2016)].

Here we present detailed results on increasing p . We use the computed values of the curves $a_{sn}(b)$ and $a_{pd}(b)$ as the starting point to increase the period, keeping b fixed. We then change b and observe that the renormalization scheme still converges nicely. In this section we report on the renormalization scheme in p .

The algorithm we used for a fixed $b = \bar{b}$ is a Newton method in three variables (x, y, a, \bar{b}) which can be stated as requirements on the periodicity in the space variables (x, y) and an extra requirement on the eigenvalue of its Jacobian matrix.

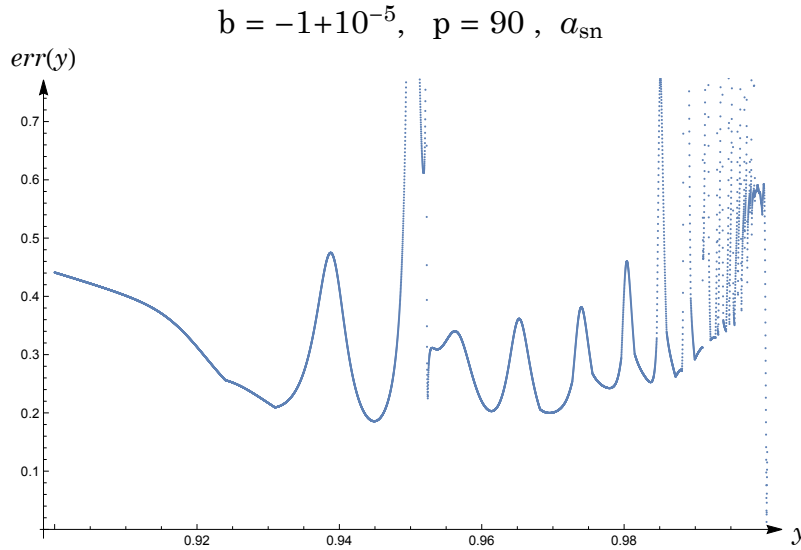


FIGURE 4. Adjustments from linear prediction in renormalization scheme. For period p initialize a Newton method with initial guess given by linear interpolation of previous $p - 1$, $p - 2$ data. If Newton’s method seems not to converge, adjust initial guess only in one variable, y and try again. This figure illustrates dependence of the final error in the calculation of a_{sn} from adjusted guess.

We look for an eigenvalue of the Jacobian matrix along the orbit to be 1 in the period-doubling case at a_{pd} and -1 for the saddle-node case at a_{sn} . As usual in Newton algorithms,

the starting point is crucial for the convergence and has to be guessed in a very precise way, especially in this case of high nonlinearity of iterated maps. The usual solution is to take random initial conditions in a certain neighborhood but we prefer to search for a renormalization approach which can predict a good guess at any step.

We start with three aligned (x, y) periodic points of orbit with consecutive periods and make a linear guess on all variables $(x(p), y(p), a(p))$ for the next period p . The error on the three conditions can vary a lot and we tried to adjust the search looking at a graph (see Fig.4) of the error as a function of one of the three variables. The error function can then be minimized by an automatic algorithm that takes advantage of its smoothness in a suitable interval (see Fig.5).

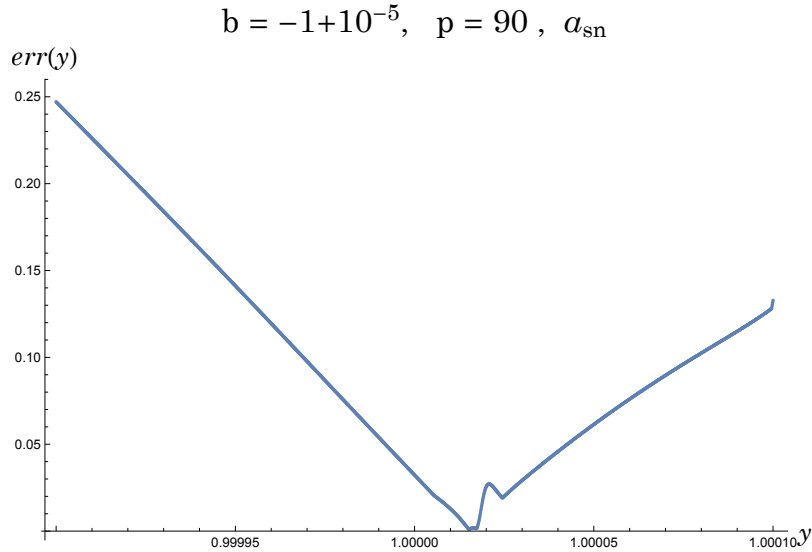


FIGURE 5. Same error function of Fig4 with period $p = 90$, $b = -1 + 10^{-5}$. The minimal error can be detected using an automatic algorithm in a suitable interval where the error function is smooth. The interval horizontal size is $2 \cdot 10^{-4}$.

In order to follow a Newton method for increasing periods is therefore very important to fix the correct branch of the orbit families. For the first low period orbits, and for symmetry reasons, the best choice is where the branch is straight, that is in the top left part of Fig.3. For higher period orbit of the family the best choice is instead near the fixed point. We have used a proper choice of branch to reach higher and higher periods. In fact once the renormalization scheme start to apply, we are able to find periodic orbits of any period with the only limitations of numerical accuracy. All calculations were done with 1000 digits precision. We got a good convergence of the algorithm for all the analyzed cases ($\varepsilon = 10^{-5}, 10^{-6}, 10^{-7}, 10^{-8}$) for periods larger than 100 near $b = 1$ and for periods larger than 50 near $b = -1$.

Some results are shown in Fig.6 (see also Fig.10 and Fig.11): the stability range of many periodic orbits is plotted with the p -periodic saddle-node bifurcation value $a_{sn}(p)$ and the

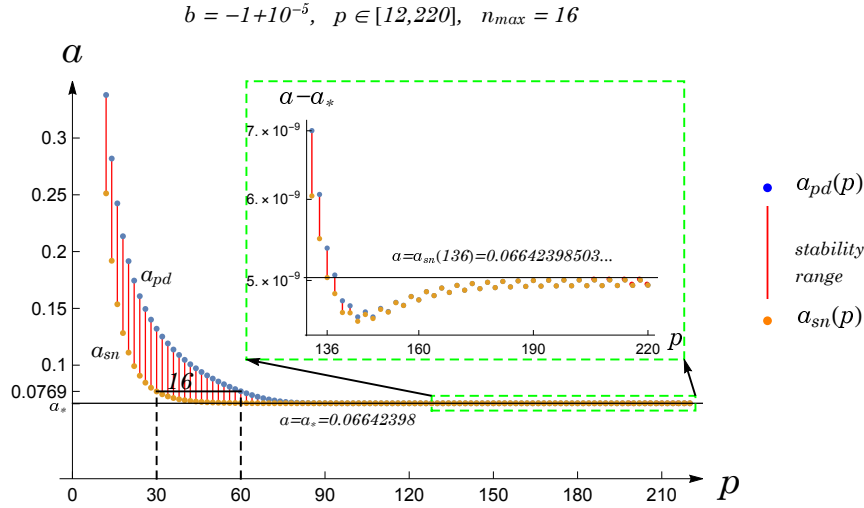


FIGURE 6. Stability ranges in the a parameter for $b = -1 + 10^{-5}$ and periodic orbits of period p between 12 and 220. For $a = .0769$ there are a maximum of 16 coexisting attractors of period p between 30 and 60. Note, in the enlarged box, the change of behavior for $p > 136$.

first period-doubling bifurcation value $a_{pd}(p)$. Note that the values $a_{sn}(p)$ and $a_{pd}(p)$ seem to decrease in p together with the corresponding stability range: in fact the stability range decreases slowly for small values of p and faster for larger values of p allowing more and more coexisting periodic attractors as $|b| \rightarrow 1$. For $b = -1 + 10^{-5}$ the maximum number of coexisting periodic attractors is 16 and can be seen for instance at $a = 0.0769$ or values of a in the interval $(0.076827, 0.077001)$ and other 7 similar intervals which satisfy the condition $a_{sn}(k) < a_{pd}(k + 15)$. For $b = -1 + 10^{-6}$ the maximum number of coexisting periodic attractors is 27 and can be seen for $a = 0.0549$ or values of a in the interval $(0.0548598, 0.0549191)$ and other 2 similar intervals which satisfy the condition $a_{sn}(k) < a_{pd}(k + 26)$. For $b = -1 + 10^{-7}$ the maximum number of coexisting periodic attractors is 39 and can be seen for $a = 0.0444$ or values of a in the interval $(0.0443212, 0.0444539)$ and other 6 similar intervals which satisfy the condition $a_{sn}(k) < a_{pd}(k + 38)$. For large p the values of $a_{sn}(p)$ and $a_{pd}(p)$ reach a minimum and then seem to remain bounded by a limiting value: for $b = -1 + 10^{-5}$ this minimum value is obtained at $p = 144$, for $b = -1 + 10^{-6}$ at $p = 188$ and for $b = -1 + 10^{-7}$ at $p = 236$. All calculations have 1000 digits of accuracy.

We show in Fig.7 coexistence of periodic attractors for certain values of a comparing the cases of $b = -1 + 10^{-5}$ and $b = -1 + 10^{-6}$. In the neighborhood of the fixed point we select a frame size which contains the outermost 15 attractive periodic orbits: for $b = -1 + 10^{-5}$ such periods p are between 32 and 60 (see also Fig.6) and for $b = -1 + 10^{-6}$ the periods p are between 66 and 94 (see also Fig.10). Note that the horizontal side length of the images,

which appear quite similar, in the two cases have different scale: periodic orbits of larger periods lies on a smaller interval of (x, y) coordinates. In the example

4. OTHER QUANTITIES AS PERIOD $p \rightarrow \infty$

4.1. Coexistence of sinks. In [Falcolini & Tedeschini-Lalli (2016)] we presented preliminary results on the case $b = 1 - \varepsilon$ and we present here the analogous results, in the quasi-conservative case, of our first paper [Falcolini & Tedeschini-Lalli (2013)].

We have analyzed the coexistence of attractors, whose number increases for $b = 1 - \varepsilon$ as ε goes to zero, and the rate of convergence of their stability range for different values of ε . As in Sec.3 we dealt with the cases $b = 1 - \varepsilon$ for $\varepsilon = 10^{-5}, 10^{-6}, 10^{-7}$ and 10^{-8} and we reached a value of $p = 120$ where the automatic Newton-method procedure applies.

4.2. Convergence regimes, changes as $\varepsilon \rightarrow 0$. We show (see Fig.8 and compare with the similar figure for $b = -1 + \varepsilon$ in [Falcolini & Tedeschini-Lalli (2013)]) that the stability range $a_{pd} - a_{sn}$ has two different rate of changement varying p : for small values of p it decreases slowly up to a certain threshold (which depends on ε) and then it reaches a renormalization-like regime where the convergence becomes exponentially fast. This behavior with two different regimes and the increasing number of coexisting attractors as ε decreases can be analyzed looking at the changes of a_{pd} and a_{sn} separately for increasing p : in Fig.9 it can be seen, for increasing value of ε , the increasing space between the curves $a_{pd}(p)$ and $a_{sn}(p)$ and the different p thresholds at which the difference $a_{pd} - a_{sn}$ becomes negligible for a limiting value $\lim_{p \rightarrow +\infty} a_{pd}(p) = \lim_{p \rightarrow +\infty} a_{sn}(p) = a_\varepsilon$ which depends on ε .

In Fig.8 we see also how the rate of convergence, with respect to the period p , of the stability range $a_{pd} - a_{sn}$ changes varying ε . The negative value of the slope m_ε in logarithmic scale increases as ε decreases which means that the stability ranges of a given p -periodic orbit becomes larger and larger approaching the conservative regime.

5. THE DISSIPATIVE STANDARD MAP

The dissipative Standard map (see for example [Schmidt & Wang (2013)]) on the cylinder, using the same notation of (1), can be written as:

$$(2) \quad T_{(a,b,\nu)}(x, y) := (a + x + \nu \sin x + b y \pmod{2\pi}, a + \nu \sin x + b y)$$

with x on a circle $\pmod{2\pi}$, constant Jacobian $0 < b \leq 1$ and the extra parameter ν as the usual perturbation parameter of the conservative Standard Map.

For the unperturbed map $\nu = 0$, and $b = 1$, the orbit with rotation number ω is invariant for changes in b if the parameter a satisfy the relation $y = \omega = \frac{a}{1-b}$ and can be followed as ν varies. For different values of ν and a given b there is an interval range of values of a at which the invariant orbit is attractive.

The differences with Hénon map (1) are great: the twist condition on the Standard map, the number of parameters; we show how to apply our method of calculations to the stability range of a periodic orbit also in this case.

A periodic orbit of rotation number $\omega = l/p$ (i.e. such that $x_p = x + l \pmod{2\pi}$) is linearly stable if the eigenvalues $\gamma_{1,2}$ of the matrix \mathbf{M}

$$\mathbf{M} = \prod_{i=0}^{p-1} \begin{pmatrix} 1 + \nu \cos x_i & b \\ \nu \cos x_i & b \end{pmatrix},$$

lie inside the unit circle. The condition on the stability range of a p -periodic orbit can then be stated also in terms of the residue \mathcal{R} defined as

$$(3) \quad \mathcal{R} = \frac{1 + \det(\mathbf{M}) - \text{tr}(\mathbf{M})}{2(1 + \det(\mathbf{M}))} = \frac{1 + b^p - \text{tr}(\mathbf{M})}{2(1 + b^p)}$$

so that a sufficient condition for an orbit of period p to be stable is

$$(4) \quad |\gamma_{1,2}| < 1 \iff 0 < \mathcal{R} < 1.$$

In a seminal paper Greene proposed, in the conservative case, a method to detect the ν threshold at which an invariant curve of irrational rotation number ω breaks down: if we let l_j/p_j be the sequence of rational approximants of ω an ω -invariant circle exists if and only if the residue $\mathcal{R}(l_j/p_j)$ is bounded.

In the paper [Falcolini & de la Llave (1992)], with Rafael de la Llave, a partial version of the Greene's method was proved. As an example of application of the method to the dissipative Standard map see [Calleja & Celletti (2010)]; for a comparative study of the conservative Hénon map, both in the orientation reversing and orientation preserving cases, with the conservative Standard map on a torus see [Miguel et al. (2013)].

In a more recent paper [Calleja & al. (2014)] a partial justification of Greene's criterion for conformally symplectic systems, including the dissipative standard map, has been given.

We show some figure for periodic orbits of rotation number $3/5$ and $8/13$ and show how their stability range depends on the parameters a, b and ν . More precisely we present in Fig.12 the space coordinates of periodic orbits which are attractive for different values of the parameter a (as in Fig.3) and in Fig.13 the curves $a_{sn}(\nu)$ and $a_{pd}(\nu)$ which gives the stability range of the $8/13$ periodic orbit as a function of ν . Such curves are evaluated using our dribbling method, starting at $b = 1$, $\nu = 0$ and fixing the coordinates (x, y) of one of the points of a 13-periodic orbit of rotation number $8/13$. We have looked for different values of b and ν and the behavior of stability range of more periodic orbits approaching the conservative case is in progress.

6. CONCLUSIONS

For the Hénon map with very small dissipation we have shown, numerical evidence of coexisting attractive periodic orbits with diverging period that have shown to accumulate approaching the conservative case. The approach is different from the perturbative approach also used in literature. We rather study the limit as the dissipation goes to zero.

As a new result, in the quasi-conservative case, we illustrate the dependence on p of the width of range of stability interval, of end points ($a_{sn}(p)$ and $a_{pd}(p)$) for periodic orbits of increasing period p is not monotone. The length of this interval decreases until it reaches a minimum, depending on b , and then it remains bounded seeming to reach an asymptote from below. Moreover, it seems to be oscillating in the orientation-reversing case, and eventually monotone in the area-preserving case. We illustrated the renormalization scheme allowing a study for large p . Using the same algorithms we discuss, as an example of applications, the stability range of periodic orbits in the dissipative Standard map.

7. ACKNOWLEDGMENTS

This research is partially supported by GNFM-INdAM.

REFERENCES

- [Calleja & Celletti (2010)] Calleja R and Celletti A "Breakdown of invariant attractors for the dissipative standard map". *Chaos*, Vol. 20, No. 1 (2010) 013121.
- [Calleja & al. (2014)] Calleja R, Celletti A, Falcolini, C. and de la Llave R. "An Extension of Greene's Criterion for Conformally Symplectic Systems and a Partial Justification". *SIAM Journal on Mathematical Analysis*, Vol. 46 (2014) 2350-2384.
- [Falcolini & de la Llave (1992)] Falcolini, C. and de la Llave R. "A rigorous partial justification of Greene's criterion". *Journal of Statistical Physics*, Vol. 67, No. 3/4, (1992) 609–643.
- [Falcolini & Tedeschini-Lalli (2013)] Falcolini, C. and Tedeschini-Lalli L. "Hénon Map: Simple Sinks Gaining Coexistence as $b \rightarrow 1$ ". *International Journal of Bifurcation and Chaos*, Vol. 23, No. 9 (2013) 1330030-1-13.
- [Falcolini & Tedeschini-Lalli (2016)] Falcolini, C. and Tedeschini-Lalli L. "Backbones in the parameter plane of the Hénon map". *Chaos: An Interdisciplinary Journal of Nonlinear Science*, Vol. 26, No. 1 (2016) 013104.
- [Gonchenko V.S. et al., 2005] Gonchenko, V.S., Kuznetsov, Yu.A. & Meijer, H.G.E. [2005] "Generalized Hénon Map and Bifurcation of Homoclinic Tangencies" *SIAM J. Appl. Dynamical Systems* **4**, 407–436.
- [Hénon(1976)] Hénon M. "A Two dimensional Mapping with a Strange Attractor" *Commun. Math. Phys.* **50**: 69-77 (1976)
- [Holmes & Whitley, 1984] Holmes, P. & Whitley, D. [1984] "Bifurcations of one- and two-Dimensional Maps" *Phil. Trans. Roy. Soc. Lond.*, **A311**: 43-102. "Erratum: Bifurcations of one- and two-Dimensional Maps" *Phil. Trans. Roy. Soc. Lond.* **A312**, 601–602.
- [Kuznetsov,1999] Kuznetsov, Yu. A. *Elements of Applied Bifurcation Theory* Springer (1999, third edition 2010)
- [Miguel et al. (2013)] Miguel, N., Simó, C. & Vieiro, A. "From the Hénon conservative map to the Chirikov standard map for large parameter values". *Regul. Chaot. Dyn.* Vol. 18, No. 5 (2013) 469–489
- [Schmidt & Wang (2013)] Schmidt, G. & Wang B.W. "Dissipative standard map". *Phys. Rev. A* Vol. 32, No. 5 (1985) 2994–2999
- [Yorke & Alligood, 1985] Yorke, J.A. & Alligood, K.T. [1985] "Period Doubling Cascades of Attractors: a Prerequisite for Horseshoes" *Comm. Math. Phys.* **101**, 305–321

8. APPENDIX

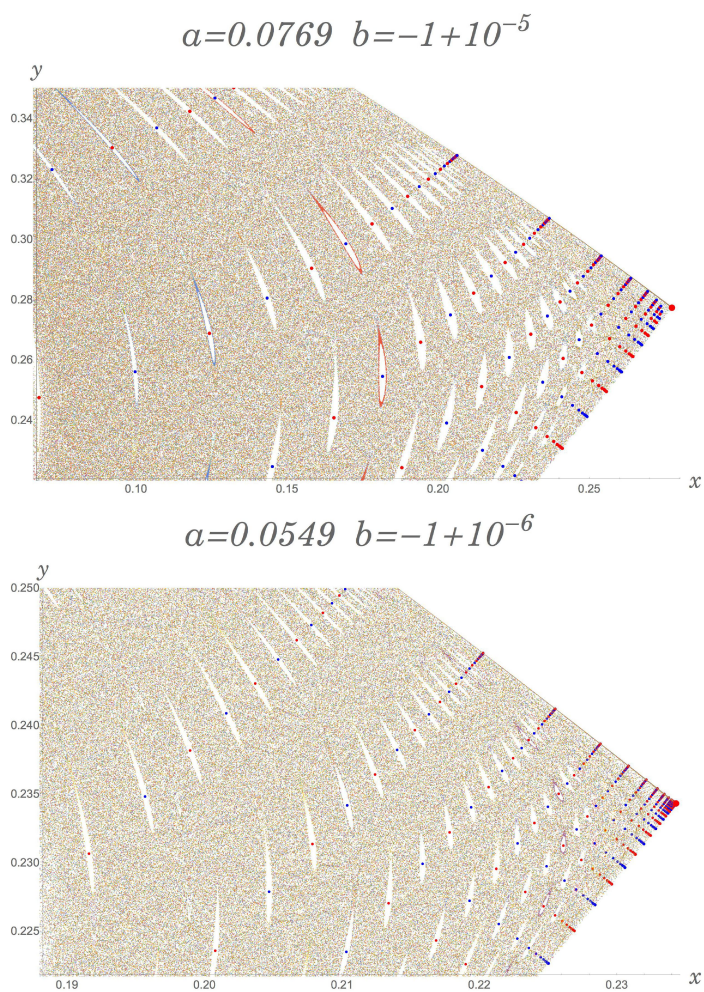


FIGURE 7. Coexistence of periodic attractors (isolated points), all other points are a unique orbit on the unstable manifold of the fixed point (rightmost big dot). Left: for $a = 0.0769$ and $b = -1 + 10^{-5}$ the horizontal side length is $2.1 \cdot 10^{-1}$. Right: for $a = 0.0549$ and $b = -1 + 10^{-6}$ the horizontal side length is $4.6 \cdot 10^{-2}$.

p	x	y	a_{sn}	$\frac{x_p}{x_{p-1}}$	$\frac{y_p}{y_{p-1}}$	$\frac{a_p}{a_{p-1}}$
12	-0.4446736408	0.4597202249	0.2512746710			
14	-0.3681763754	0.3453287622	0.1919397498	0.8279698674	0.7511715680	0.7638642965
16	-0.2655588696	0.2940788855	0.1536385892	0.7212816664	0.8515910566	0.8004521699
18	-0.1825154895	0.2757119770	0.1282813066	0.6872882452	0.9375442804	0.8349549892
20	-0.1177028837	0.2751192136	0.1110820980	0.6448925734	0.9978500627	0.8659258389
22	-0.06776115069	0.2825656841	0.09914904099	0.5756966063	1.027066341	0.8925744360
24	-0.02936152052	0.2928153913	0.09069761229	0.4333090601	1.036273715	0.9147603585
26	0.0002411967946	0.3033264883	0.08460266177	-0.008214724250	1.035896668	0.9327992175
28	0.02316601016	0.3129895520	0.08013863254	96.04609465	1.031856973	0.9472353572
30	0.04100722744	0.3214097547	0.07682696335	1.770146311	1.026902504	0.9586757462
32	0.05495508983	0.3285298392	0.07434482451	1.340131808	1.022152671	0.9676918268
34	0.06589974700	0.3344402271	0.07246963941	1.199156388	1.017990414	0.9747771938
36	0.07451145457	0.3392862637	0.07104470729	1.130678917	1.014489993	0.9803375298
38	0.08129967732	0.3432245046	0.06995754264	1.091103077	1.011607428	0.9846974576
40	0.08665560833	0.3464032369	0.06912596741	1.065878872	1.009261379	0.9881131441
42	0.09088254823	0.3489547883	0.06848903032	1.048778607	1.007365842	0.9907858491
44	0.09421759672	0.3509934165	0.06800095540	1.036696248	1.005842098	0.9928736775
46	0.09684729910	0.3526157651	0.06762703208	1.027910947	1.004622163	0.9945012049
48	0.09891907374	0.3539024084	0.06734075520	1.021392178	1.003648854	0.9957668276
50	0.1005497298	0.3549197897	0.06712179354	1.016484749	1.002874751	0.9967484526
52	0.1018319239	0.3557222095	0.06695450969	1.012751841	1.002260848	0.9975077565
54	0.1028391582	0.3563537113	0.06682686399	1.009891144	1.001775267	0.9980935460
56	0.1036296920	0.3568497862	0.06672958567	1.007687090	1.001392085	0.9985443230
58	0.1042496494	0.3572388746	0.06665554203	1.005982430	1.001090342	0.9988903928
60	0.1047354902	0.3575436563	0.06659925095	1.004660359	1.000853160	0.9991554928
62	0.1051159936	0.3577821444	0.06655650571	1.003632994	1.000667018	0.9993581724
64	0.1054138396	0.3579685944	0.06652408239	1.002833498	1.000521127	0.9995128453
66	0.1056468793	0.3581142564	0.06649951490	1.002210712	1.000406913	0.9996306977
68	0.1058291430	0.3582279864	0.06648091878	1.001725216	1.000317580	0.9997203571
70	0.1059716488	0.3583167423	0.06646685693	1.001346565	1.000247764	0.9997884829
72	0.1060830382	0.3583859811	0.06645623402	1.001051125	1.000193234	0.9998401774
74	0.1061700863	0.3584399779	0.06644821707	1.000820565	1.000150667	0.9998793649
76	0.1062380982	0.3584820770	0.06644217251	1.000640594	1.000117451	0.9999090336
78	0.1062912288	0.3585148934	0.06643761980	1.000500109	1.000091543	0.9999314786
80	0.1063327276	0.3585404693	0.06643419400	1.000390425	1.000071338	0.9999484359
82	0.1063651378	0.3585603997	0.06643161907	1.000304799	1.000055588	0.9999612408
84	0.1063904464	0.3585759287	0.06642968556	1.000237941	1.000043309	0.9999708948
86	0.1064102083	0.3585880275	0.06642823555	1.000185749	1.000033741	0.9999781721
88	0.1064256372	0.3585974528	0.06642714921	1.000144994	1.000026284	0.9999836465
90	0.1064376827	0.3586047950	0.06642633657	1.000113183	1.000020475	0.9999877664
92	0.1064470856	0.3586105140	0.06642572928	1.000088342	1.000015948	0.9999908577
94	0.1064544257	0.3586149687	0.06642527629	1.000068955	1.000012422	0.9999931806
96	0.1064601546	0.3586184381	0.06642493873	1.000053815	1.000009675	0.9999949182
98	0.1064646262	0.3586211404	0.06642468779	1.000042003	1.000007535	0.9999962222
100	0.1064681158	0.3586232448	0.06642450139	1.000032777	1.000005868	0.9999971937
102	0.1064708394	0.3586248838	0.06642436338	1.000025581	1.000004570	0.9999979224
104	0.1064729645	0.3586261600	0.06642426123	1.000019959	1.000003559	0.9999984622
106	0.1064746230	0.3586271540	0.06642418600	1.000015577	1.000002772	0.9999988673
108	0.1064759169	0.3586279279	0.06642413053	1.000012151	1.000002158	0.9999991650
110	0.1064769267	0.3586285306	0.06642408995	1.000009484	1.000001681	0.9999993890
112	0.1064777143	0.3586289999	0.06642406016	1.000007396	1.000001308	0.9999995515
114	0.1064783290	0.3586293653	0.06642403856	1.000005774	1.000001019	0.9999996749
116	0.1064788083	0.3586296498	0.06642402278	1.000004501	1.000000793	0.9999997624
118	0.1064791825	0.3586298714	0.06642401148	1.000003514	1.000000618	0.9999998300
120	0.1064794741	0.3586300438	0.06642400326	1.000002738	1.000000481	0.9999998762
122	0.1064797019	0.3586301782	0.06642399749	1.000002139	1.000000375	0.9999999132
124	0.1064798792	0.3586302827	0.06642399329	1.000001665	1.000000291	0.9999999368
126	0.1064800179	0.3586303641	0.06642399045	1.000001302	1.000000227	0.9999999572
128	0.1064801257	0.3586304274	0.06642398837	1.000001012	1.000000176	0.9999999686
130	0.1064802101	0.3586304769	0.06642398705	1.000000793	1.000000138	0.9999999801
132	0.1064802756	0.3586305152	0.06642398605	1.000000615	1.000000107	0.9999999849
134	0.1064803270	0.3586305452	0.06642398549	1.000000483	1.000000084	0.9999999917

TABLE 1. $b = -1 + 10^{-5}$. For each period p : (x, y) space coordinates of initial point, a_{sn} value of saddle-node bifurcation. Ratio of these values with consecutive periods.

p	x_{in}	y_{in}	first eigenvalue	accuracy
42	-0.02471212033	-0.004353351966	0.999666+0.025007 i	980
44	0.003893968151	0.01400370243	0.998106+0.061164 i	981
46	0.03287883220	0.03630238615	0.996571+0.082467 i	981
48	0.06028145342	0.05973990689	0.994655+0.103021 i	980
50	0.08552343060	0.08300646446	0.992221+0.124292 i	980
52	0.1082722485	0.1051821971	0.989124+0.146904 i	979
54	0.1283734421	0.1256447760	0.985195+0.171279 i	979
56	0.1458237800	0.1440274072	0.980218+0.197778 i	979
58	0.1607392037	0.1601751773	0.973924+0.226748 i	979
60	0.1733182271	0.1740957680	0.965971+0.258534 i	979
62	0.1838069083	0.1859098749	0.955930+0.293489 i	979
64	0.1924697936	0.1958070451	0.943258+0.331965 i	978
66	0.1995685673	0.2040103236	0.927268+0.374309 i	978
68	0.2053481559	0.2107505750	0.907097+0.420841 i	978
70	0.2100289888	0.2162495981	0.881651+0.471827 i	978
72	0.2138038071	0.2207103044	0.849555+0.527432 i	978
74	0.2168375173	0.2243120570	0.809070+0.587650 i	979
76	0.2192688855	0.2272094757	0.758004+0.652192 i	979
78	0.2212131915	0.2295333706	0.693593+0.720313 i	979
80	0.2227652522	0.2313928385	0.612348+0.790538 i	979
82	0.2240024479	0.2328778729	0.509870+0.860204 i	978
84	0.2249875438	0.2340620792	0.380610+0.924690 i	977
86	0.2257712060	0.2350052607	0.217565+0.976002 i	977
88	0.2263941791	0.2357557547	0.011907+0.999885 i	976
90	0.2268891314	0.2363524720	-0.247504+0.968841 i	975
92	0.2272821942	0.2368266348	-0.574717+0.818296 i	975
94	0.2275942304	0.2372032327	-0.987457+0.157593 i	974
96	0.2278418727	0.2375022270	-0.379187	974
98	0.2280383657	0.2377395373	-0.244788	973

TABLE 2. For the coexisting attractive periodic orbits in Fig.7 for $b = -1 + 10^{-6}$ and $a = 0.0549$ we list the period, the first 10 digits of the space coordinates of initial point, the corresponding eigenvalue of the Jacobian matrix along their orbit and the precision accuracy of the calculation. The first 27 orbits, with period from 42 to 94, are attractors with complex eigenvalues.

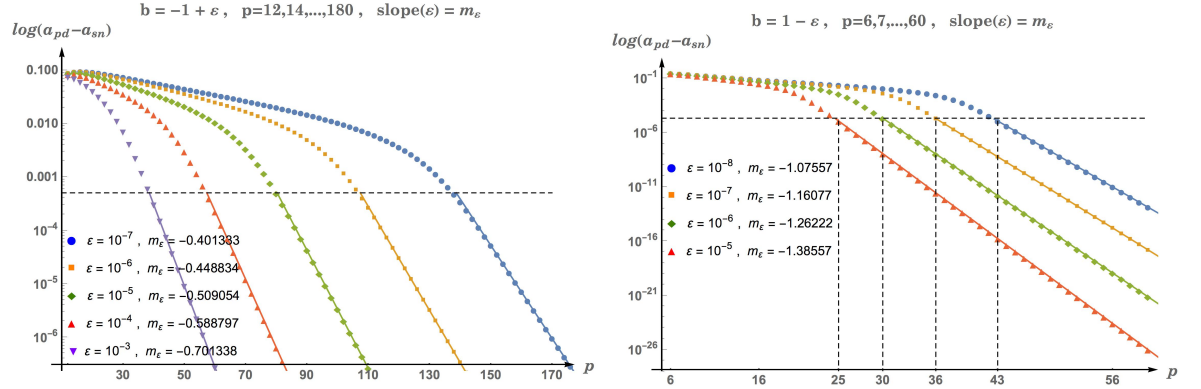


FIGURE 8. Rate of convergence in p of the stability range $a_{pd} - a_{sn}$. Left: $b = -1 + \epsilon$ with $\epsilon = 10^{-3}, 10^{-4}, 10^{-5}, 10^{-6}$ and 10^{-7} . Right: $b = 1 - \epsilon$ with $\epsilon = 10^{-5}, 10^{-6}, 10^{-7}$ and 10^{-8} . The negative value of the slope m_ϵ in logarithmic scale increases as ϵ decreases.

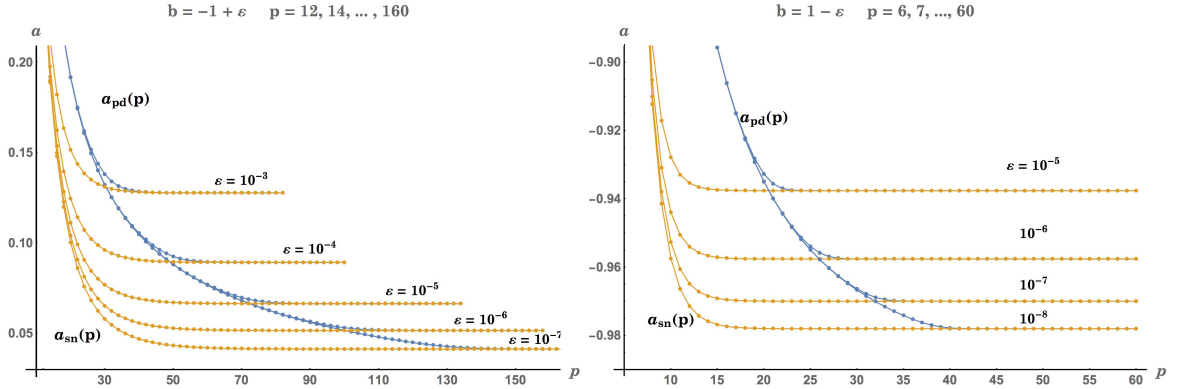


FIGURE 9. Values of $a_{pd}(p)$ and $a_{sn}(p)$. Left: $b = -1 + \epsilon$ with $\epsilon = 10^{-3}, 10^{-4}, 10^{-5}, 10^{-6}$ and 10^{-7} . Right: $b = 1 - \epsilon$ with $\epsilon = 10^{-5}, 10^{-6}, 10^{-7}$ and 10^{-8} .

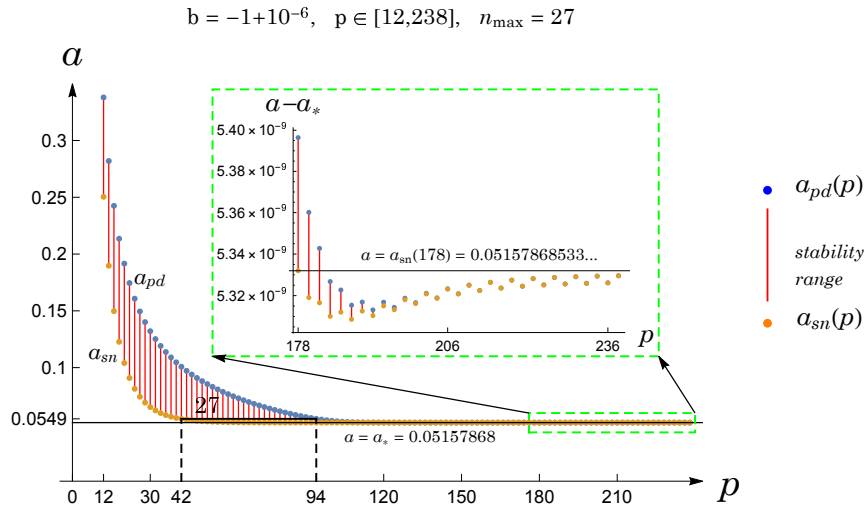


FIGURE 10. Stability ranges in the a parameter for $b = -1 + 10^{-6}$ and periodic orbits of period p between 12 and 238. For $a = .0549$ there are a maximum of 27 coexisting attractors of period p between 42 and 94. Note, in the enlarged box, the change of behavior for $p > 178$.

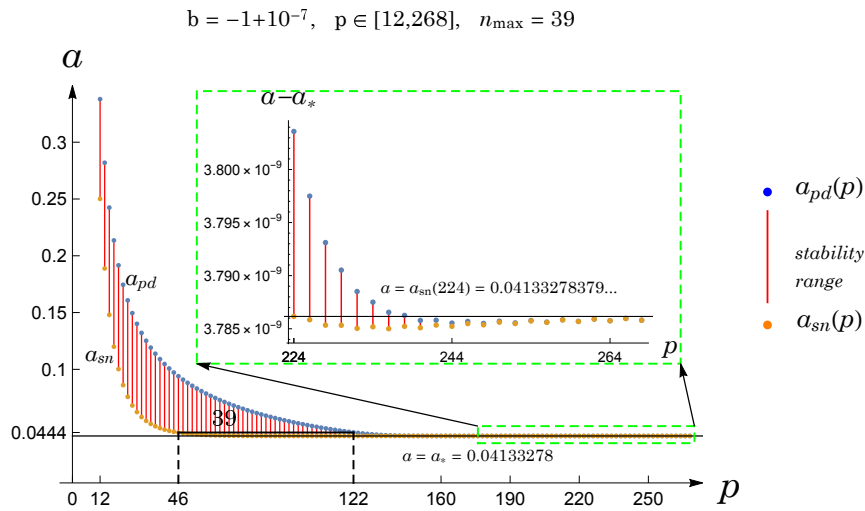


FIGURE 11. Stability ranges in the a parameter for $b = -1 + 10^{-7}$ and periodic orbits of period p between 12 and 268. For $a = .0444$ there are a maximum of 39 coexisting attractors of period p between 46 and 122. Note, in the enlarged box, the change of behavior for $p > 224$.

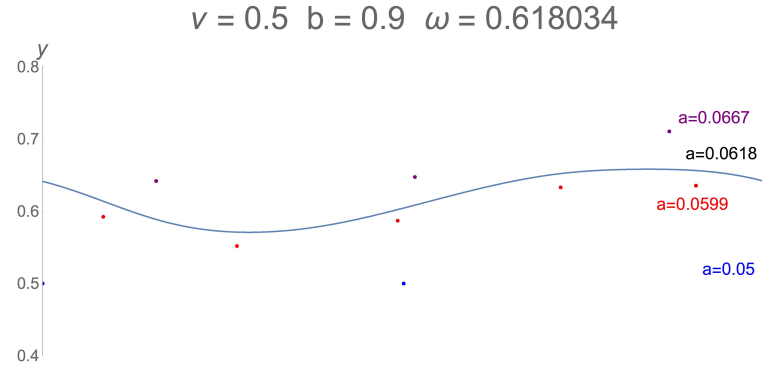


FIGURE 12. For $b = 0.9$ and $\nu = 0.5$ an invariant attractor with an irrational rotation number ω and the approximating periodic orbits $1/2$, $2/3$, $3/5$, $5/8$ which are attractive for different values of a .

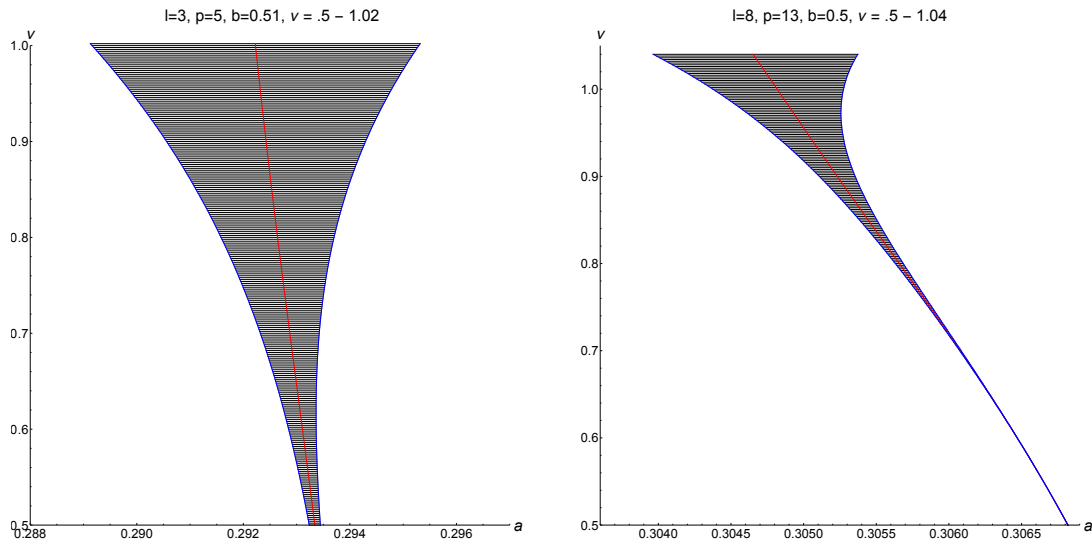


FIGURE 13. Stability range in (a, ν) , $b = 0.5$, for two periodic orbits with rotation number $\omega = 3/5$ and $\omega = 8/13$. The border curves corresponds to the values of $a_{sn}(\nu)$ and $a_{pd}(\nu)$. The middle curve corresponds, given b and ν , to values of a for which the residue is maximum.